Available online at www.sciencedirect.com

SciVerse ScienceDirect

Physics Procedia 42 (2013) 154 – 162

Physics Procedia

PNCMI 2012 - Polarized Neutrons for Condensed Matter Investigations 2012

Polarization analysis with ^{3}He spin filters for separating coherent from incoherent scattering in soft matter studies

E. Babcock [1a], Z. Salhi[a,b], M-S. Appavou[a], A. Feoktystov[a], V. Pipich[a], A. Radulescu[a], V. Ossovyi[a], S. Staringer[a], A. Ioffe[a]

[a] *Juelich Centre for Neutron Science, Lichtenbergstr 1., Garching, 85747, Germany*
[b] *ESS design Update, German Contribution*

Abstract

In soft matter small angle neutron scattering (SANS) studies at large Q values, incoherent scattering becomes the dominant signal. In the Q-range of interest to this work, from 0.2 Å^{-1} to about 1.0 Å^{-1}, the coherent scattering from the typical protein or polymer in a D_2O buffer solution inevitably drops one to two orders of magnitude or more below the total scattering. Even after careful and accurate subtraction of the measured D_2O buffer scattering, the remaining corrected, i.e. sample-only, signal will still be dominated by diffuse incoherent scattering from hydrogen in the sample itself. This is the exact region of interest when one wishes to probe the structural changes in "living" proteins caused by interactions and motions related to function. To further complicate the problem, there is strong motivation to measure this Q-regime at very low concentrations because it has been shown with wide angle X-ray scattering that proteins can undergo concentration-dependent structural changes that rapidly increase below concentrations of about 5% [1] motivating the study of protein solutions at ever lower concentrations. In this case the signal from the protein will inevitably become much less than the scattering of the D_2O buffer solution it is contained in. Polarization analysis offers the opportunity to separate the weak coherent signal from the larger incoherent signal and perhaps enable measurements under the conditions described above. This paper will address the issues associated with the correct separation of coherent and incoherent scattering for soft matter samples. We have performed tests measurements on KWS2 which show the viability of the method on a protonated α-lactalbumin solution at 2.5% (1 mm thick) and 0.25% (2 mm thick) concentrations in a D_2O buffer solution. Additionally describe a the method of implementation using ^{3}He spin filters, some practical considerations, and future plans for a dedicated device at the JCNS.

Selection and peer-review under responsibility of the Organizing Committee of the 9th International Workshop on Polarised Neutrons in Condensed Matter Investigations

Keywords: polarized neutrons, incoherent background, SANS, SEOP, polarized ^{3}He

1. Introduction

When applied to soft matter studies, polarization analysis (PA) can be used to separate coherent and incoherent contributions of the total scattering curve. The incoherent scattering in the case of biological

[1] Email: e.babcock@fz-juelich.de

1875-3892
Selection and peer-review under responsibility of the Organizing Committee of the 9th International Workshop on Polarised Neutrons in Condensed Matter Investigations
doi:10.1016/j.phpro.2013.03.190

samples is caused mainly by hydrogen atoms because they have a very large incoherent cross section of 80 barn per atom, and always constitute a significant part of the atoms in any protein, polymer or biological molecule. The latter cross sections should be compared with coherent cross sections of the other most abundant constituents of such molecules: 5.5 barn for carbon, 11 barn for nitrogen and 4.2 barn for oxygen per atom. Consequently, the hydrogen atoms in such biological molecules are strong intrinsic sources of incoherent scattering which can be larger than the coherent scattering from the sample. This is especially the case for what we consider to be the high Q-range accessible by SANS, i.e. from about 0.2 Å^{-1} to 1.0 Å^{-1}. To further complicate matters, as it will be justified below, it could be very desirable to measure extremely low concentrations of proteins in D_2O buffer solutions, in which case the desired coherent signal of the dilute sample can be 2 orders of magnitude or more below the total scattering of the sample-D_2O buffer mixture in the high Q-regime. The utility of PA for soft matter samples is thus to increase the fidelity of the coherent signal in this Q-regime and hopefully to enable structure measurements of active proteins under conditions very difficult or impossible to access with other available methods.

Wide angle X-ray scattering, which is insensitive to the scattering from the light hydrogen atoms, can also be used to probe this Q-range, and indeed important structural changes in proteins have been observed with this method as one decreases the concentration of the samples below about 5% , however the method can run into limits at even lower concentrations[2, 3]. Conversely, while with SANS it is proposed to measure low concentration samples in this Q-regime, because of the sensitivity of neutron scattering to the large incoherent cross section of the hydrogen atoms in the sample, and because of the incoherent scattering of the D_2O buffer solution being much larger than the coherent scattering signal of interest, one runs into other limits. For example, the buffer scattering must be subtracted to increasingly higher accuracy in order to be able to see signals say 1% or lower of the total scattering with sufficient statistics [4, 5]. Also, even when one can subtract the buffer scattering to sufficient accuracy, because of systematic errors in the absolute calibration of the measured scattered intensity, the subtraction of an analytically calculated incoherent sample background could be problematic. Further, improper coefficients for the incoherent background can lead to errors in other parts of the structure analysis [6, 7].

Neutron polarization analysis is another way to address this problem. Using a polarized incident neutron beam and analyzing the spin state of the scattered neutrons one can distinguish between the coherent and incoherent components [8]. This effectively raises the fidelity of the measurement by looking at the coherent scattering separately. Recently we have applied this method in an experiment carried out on the SANS diffractometer KWS2 of the JCNS at the FRM II in Garching (Germany) [9]. We studied the structure of lactalbumin at 2.5% and 0.25% concentrations in a D_2O buffer solution (pH7). Further, we have performed time of flight measurements in order to address the problem of proper data corrections caused by the nuetron wavelength dependent efficiencies of the ^{3}He neutron spin analyzer cell and detector, which could be affected by the inelastic up-scattering of neutrons caused by our hydrogen-containing samples [10]. Finally we propose a way to further increase our measurable Q-range all the way to 1Å^{-1} while using a dedicated ^{3}He spin filter device optimized for routine use.

2. Method of PA for separation of coherent from incoherent scattering

The method of PA for soft matter samples using a polarized ^{3}He neutron spin filter has been described previously [11]. We point out that the discussion here is only valid for scattering in which there is no magnetic component, thus all the spin flip scattering arises from the well known 2/3 spin flip probability of spin-incoherent scattering [8]. Further, our discussion is simplified by the fact that we use an AFP ^{3}He flipper to reverse the ^{3}He spin state, thus no corrections for flipping efficiency are required because the ^{3}He has a symmetric analyzing power regardless of the analyzer spin state for equal values of ^{3}He polarization [12].

To perform PA for separation of coherent scattering, the important parameters are the measured asymmetry of the beam scattered from the sample, A_s, and the instrument asymmetry or analyzing power without the sample, A_0.

$$A_{s(\text{or})0} = \frac{N_p - N_a}{N_p + N_a} \tag{1}$$

Here N_p and N_a are simply the neutron count rates in the orientation where the incident beam polarization and ^{3}He polarization are parallel and anti-parallel respectively. For A_0, in the case when the incident beam polarization is parallel to the ^{3}He polarization there is high neutron transmission and for anti-parallel polarization low transmission. Thus A_0 is positive and equal to the total instrument analyzing power or product of the incident beam polarization and the ^{3}He analyzing efficiency. However, for spin-incoherent scattering, since neutrons have a 2/3 spin-flip scattering probability, A_s is actually negative when the spin-incoherent scattering is dominant. In principle one should calibrate A_0 over the detector area, or as a function of Q, however for ^{3}He cells with good geometry, these corrections are of a cosine nature and typically small [13], especially for the case of an opaque neutron spin filter (i.e. a spin filter with analyzing efficiency > 99 %) as was used in this work. Thus we simply measured A_0 for the attenuated direct beam passing through the center of the cell in this work.

Once these two asymmetries are known one can easily derive the spin-flip N_{SF} and non-spin-flip N_{NSF} fractions.

$$N_{SF} = N_T \frac{A_0 + A_s}{2A_0} \quad (2) \qquad \text{and} \qquad N_{NSF} = N_T \frac{A_0 - A_s}{2A_0} \quad (3)$$

where N_T is the total scattering or the sum of $N_p + N_a$. Now one can simply calculate the spin coherent scattering N_{coh}, and the spin incoherent scattering N_{incoh} as

$$N_{incoh} = \frac{1}{p} N_{SF} \quad (4) \qquad \text{and} \qquad N_{coh} = N_{NSF} - \frac{1-p}{p} N_{SF} \quad (5)$$

where p is the spin flip probability factor for the scattered beam which is 2/3 for incoherent single scattering [8]. For pure incoherent neutron scattering, in the single scattering limit, one can see the measured A_s would be -1/3 for a perfect $A_0 = 1$. In this case one arrives at the well known $N_{SF} = 2/3$, and $N_{NSF} = 1/3$ directly. Note that this corresponds to a neutron flipping ratio $F = (1 + A_s)/(1 - A_s) = 1/2$. However for doubly scattered neutron the A_s would be +1/9 [8]. Thus for samples with multiple scattering, (i.e. for non-absorbing samples with transmissions deviating from unity) the multiple scattering fraction should be estimated or modeled from the transmission value in order to obtain the correct p. For an estimate of p, we assume a non-absorbing sample so that the loss in transmission, or attenuation a, is caused solely by multiple scattering. We also assume that we can approximate the solution close to the single scattering limit only considering 2$^{\text{nd}}$ order scattering events. Given an attenuation $a = 1 - T$, where T is the beam transmission, the transmitted beam asymmetry A_2 would be,

$$A_2 = -(1 - a)(1/3) + a(1/9) \quad (6)$$

and then using the definition of A_s in Eq. 1 and since $N_p = 1 - p$ and $N_a = p$ one arrives at the spin flip probability p with multiple scattering of

$$p = (1 - A_2)/2. \quad (7)$$

Although this estimate is crude, we arrive at perhaps fortuitously good agreement using this analytical model to the monte-carlo modeling result of [11] which is discussed further in section 3.

Multiple scattering changing the p-factor is not the only correction one must consider. Ghosh and Rene showed that inelastic scattering of soft matter samples can lead to errors in the absolute calibration of cross sections if careful attention is not paid to how one calibrates and corrects the data [10] thus this effect must be taken into account. Luckily, for the method of polarization analysis using a ^{3}He spin filter, the wavelength dependent analyzing efficiency is highly deterministic and can easily be integrated once the sample-transmitted neutron spectrum is known. Therefore we performed time-of-flight (TOF) tests also on KWS2 [9]. A small 50 Hz disc chopper was installed near the sample position to chop the 4.55 Å wavelength neutron beam. Data were then acquired in TOF mode for 2 hours for each sample. The data were analyzed by placing a generous data mask around the direct beam to reject any low-Q non-diffuse scattering or beam induced background, and then summing the un-masked detector counts as a function of TOF. Shown in figure 1 are the obtained TOF spectra for 1 mm and 2 mm thickness of water and 1.5 mm of plexiglass. One can see that the inelastic scattering fraction at this resolution is similar but not identical for the two

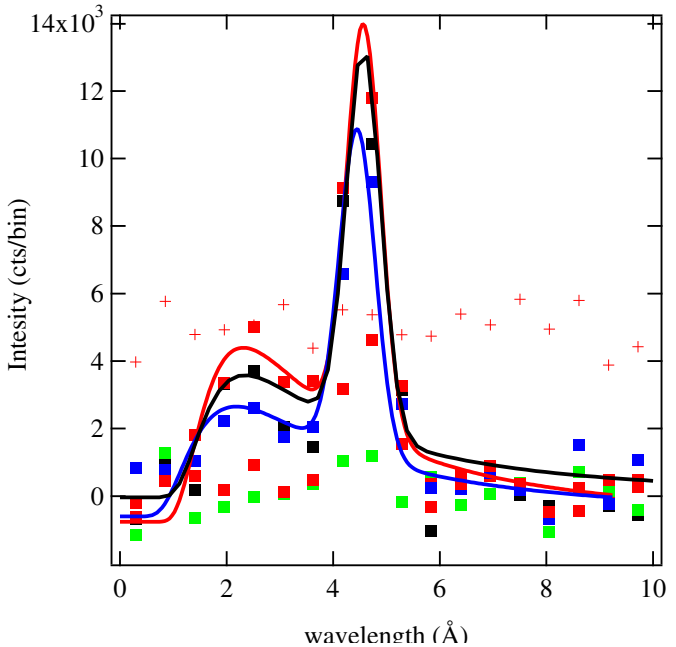

Fig. 1. Measured time of flight spectra with a chopper near the sample position. Spectra shown are for strong incoherent scatters, 1 mm H_2O (blue), 2 mm H_2O (red) and 1.5 mm plexi glass (black) after the empty beam background is subtracted. The solid lines are fits using a Gaussian of fixed position and width corresponding to our velocity selector parameters convoluted with a Maxwell-Boltzmann distribution. The Maxwellian and Gaussian amplitudes, the Maxwellian temperature, and a constant background were free parameters. The points of the same color are the corresponding data. The green points are an attempted measurement of our protein in a D_2O buffer, and the red crosses are the empty cell.

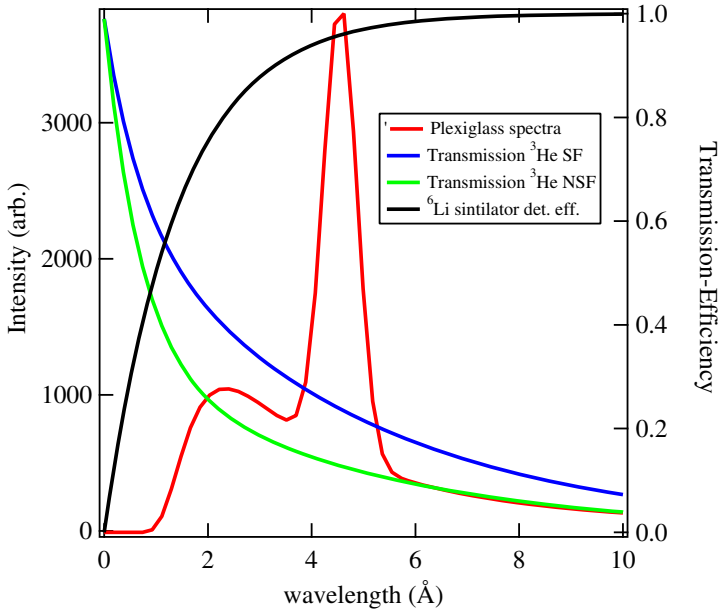

Fig. 2. Comparison of the fit time of flight spectra of the Plexiglass sample with the respective Li sintillator detector efficiency and the ^{3}He transmissions for a pure incoherent scattered signal using a ^{3}He cell with 11.4 bar-cm ^{3}He and 68% polarization with an incident beam polarization of 93% . Note for perfect analyzing, polarizing, and detector efficiencies the ratio of the blue to green lines, would be 2 for pure spin-incoherent scattering, which corresponds to the measured flipping ratio F=1/2=NSF/SF.

very different samples. Unfortunately we could not obtain reliable data on the D_2O buffer solution, as its scattering is approximately one order of magnitude lower than either plexiglass or water.

However, if we assume that plexiglass would represent a typical worse-case scenario of the inelastic scattering from a protein in solution, we can already make an estimate of how large of a correction must be made in order to properly analyze the data without significant systematic errors due to the inelastic scattering. Using the measured TOF curve for plexiglass and the calculated ^{3}He transmission, for the pressure length product and actual polarization of the ^{3}He cell we used, along with the known detector efficiency over wavelength as shown in figure 2, we can numerically integrate the actual A_0 for the TOF spectrum. For this data we arrive at a total analyzing efficiency when the signal is dominated by incoherent scattering of 85.6% whereas the total analyzing power for coherently scattered neutrons, which should have negligible inelastic scattering, and which dominate the scattering curve at low Q, was measured to be 92.1% for the 4.55Å incident beam. For the case of H_2O and plexiglass the scattering is purely incoherent and isotropic over our Q-range and one should use $A_0 = 85.6\%$ for this data. When there is a mixture of coherent and incoherent scattering one should use an analyzing efficiency of

$$A_0 = A_0^o - \Delta A \frac{N_{incoh}}{(N_{coh} + N_{incoh})} \tag{8}$$

where A_0^o is the measured instrument analyzing efficiency of the incident beam and analyzer, and ΔA is determined from numerical integration of the product of the normalized N_{incoh} TOF spectrum, detector efficiency, and the respective ^{3}He transmission of the spin flip and non spin flip signals for our incident beam polarization as summarized visually in figure 2. ΔA again as determined from the information given in 2 is 6.5% . This correction, if not made, would then lead to an error in the deduced N_{incoh} of about 2.5% . Thus the correction would become critical to determination of the absolute magnitude of N_{coh} as it becomes much smaller than the N_{incoh} of the sample.

3. Test measurement on a Lactalbumin sample in a deuterated buffer

In order to test the method we used a provisionary setup, shown in figure 3. A shielded and end compensated 35 cm long solenoid was used to maintain a highly uniform magnetic field for our ^{3}He cell. Within this solenoid, the 6 cm diameter cell called "J8," which has a length of 6 cm and ^{3}He pressure of 2.1 bar (at room temperature), was placed on a mount in the center and a single sample cell holder was used to place the sample approximately 1 cm in front of the ^{3}He cell inside of the solenoid. A transverse RF field for AFP flipping of the ^{3}He polarization was created via. a pair of 8 cm x 8 cm square coils approximately 7 cm apart around the cell driven by a house built power amplifier (200 W and V_{pp}=130 V from 1-100 kHz). The AFP RF burst was performed using the same computer synthesized waveform as described in [12]. Achieved losses were approximately $2x10^{-5}$ per flip, thus given the number of flips required for this measurement there were no measurable losses due to the AFP spin flipping. The polarization decay time constant of the J8 cell was over 200 hours in this configuration. Thus given the 5 hour total time of this experiment, we experienced less than a 2 % total change in the ^{3}He polarization which had a starting value of 67.9 %. The incident beam on KWS2 is polarized via. a transmission super mirror polarizer placed in the 2 m collimation section just before the sample slits. This polarizer provided a 92.8 % polarizing efficiency for the 4 m beam collimation (i.e. final beam divergence defining aperture at 4 m from the sample position) and the 4.55 Å neutron wavelength used for this experiment [14].

Alpha-lactalbumin from bovine milk was purchased from Sigma-Aldrich (ref: L 5385). Phosphate salts (Na_2HPO_4 and NaH_2PO_4) were provided by Merck (ref: K37807280 744 and A723946 742 respectively). All salts were H/D exchanged according to a process described by Calmettes et al [15]: each salt is dissolved in pure D_2O and left overnight for H/D exchange. Then the D_2O is removed from the salt solution by being heated at 60 °C under vacuum. This procedure is repeated five times. Deuterated phosphate buffer was prepared by mixing the obtained Na_2DPO_4 and NaD_2PO_4 salts in D_2O order to have pD = 7.0, knowing that pD = pH read + 0.41 [16]. The final buffer solution is filtered using 0.22 μm filter to remove eventual dusts before use. The lyophilized alpha-lactalbumin powder was dissolved and dialyzed four times against

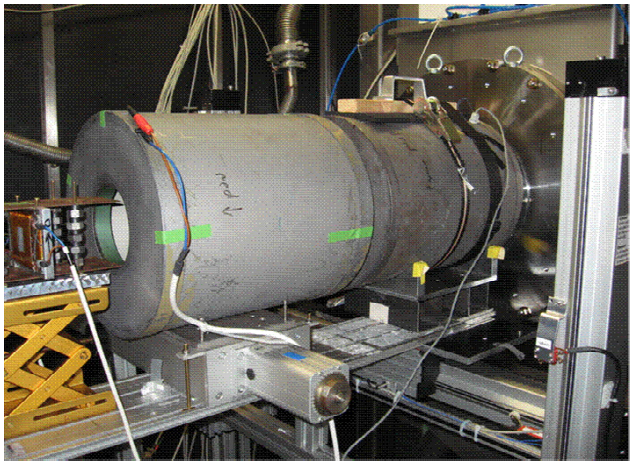

Fig. 3. A photo of the provisionary setup. The system uses cells polarized externally in the lab and transported to the beam. The first solenoid is simply to provide adiabatic rotation from the vertical guide fields to the longitudinal ^{3}He holding field. Lifetime with a typical ^{3}He cell is over 200 hours. The sample is in a holder placed directly before the cell to give a large Q range with a typical 6 cm diameter cell. An RF coil is mounted around the cell in order to perform AFP flipping of the ^{3}He polarization. For non-magnetic samples no other spin flipper is required.

the deuterated phosphate buffer at pD 7.0 for removing eventual conservative products and performing H/D exchange of the labile protons. The dialysis process was performed by using a dialysis cassette of 3 mL volume with 3 kDa MWCO membrane pores, purchased from the Pierce Company, in 300 mL deuterated phosphate buffer at pD 7.0. The solution was centrifuged at 20000 g at 4 °C during 1 hour to remove eventual aggregates. The protein concentration was measured by UV spectroscopy using the alpha-lactalbumin molar extinction coefficient at 280 nm = 24450 $M^{-1}cm^{-1}$ (i.e. 1.5 L $g^{-1}cm^{-1}$). The initial concentration obtained was 25.38 mg mL^{-1} (2.5%) and diluted ten times to obtain a dilute solution at 2.54 mg mL^{-1} (0.25%) for our measurements.

The 2.5% sample was in a 1 mm thick cell and the 0.25% sample in a 2 mm cell. Corresponding 1 mm and 2 mm thick cells with just the deuterated buffer were also prepared. The total measurement involved measuring the spin flip and non spin flip scattering from the two Lactalbumin and the two corresponding buffer solutions plus a 1 mm H_2O sample. This was followed by an absolute instrument calibration performed via measurement of a 1.5 mm thick plexiglass sample as a secondary calibration standard, a boron carbide absorber to measure non/beam related background, an empty sample cell, and the empty beam. This procedure is the standard means for making SANS measurements in absolute units. Since the plexi-glass sample fully depolarizes the beam due to multiple scattering, the calibration count rates were scaled by the numerically integrated ratio of ^{3}He transmission, including the measured inelastic scattering, for the polarization of the incident beam to that of an unpolarized beam, a factor of 1.81 in this case. Typically each spin state was measured for about 15 minutes. At the end of the measurement, the incident beam polarizer was removed and the absolute transmission vs. wavelength of the ^{3}He cell was measured with the ^{3}He polarized and then unpolarized at three wavelengths, 4.5 Å, 7 Å and 10 Å, in order to calibrate the ^{3}He density length product and absolute polarization [17]. The total time for the measurements was about 5 hours.

Radial integration as a function of Q was carried out with the QtiKWS software package [18]. We first analyzed the scattering separately for the two spin states of each sample in absolute units. Then to prevent problems due to possible corrections of A_0 due to inelastic effects and also changes in p due to multiple scattering in the buffer, the properly volume faction normalized count intensities from the buffer were subtracted from the intensities of the buffer-sample solutions. After this subtraction, polarization analysis was performed on the sample-only intensity to give the curves shown in figure 4. For the incoherent scattering curves of the H_2O and the D_2O buffer, the p-factors were corrected for multiple scattering using our estimate of multiple scattering based on the measured sample transmission values T as described in Eqs. 6, 7. Using this approximation the p-factors used for the scattering curves were 0.648, 0.628 and 0.566 for the 1 mm D_2O, 2 mm D_2O, and 1 mm H_2O samples respectively where the corresponding measured transmissions were 0.915, 0.828 and 0.545. We quickly note that this very crude estimate gives perhaps fortuitously good agreement with the value of $p = 0.630$ for $T = 0.833$ calculated via monte-carlo simulations in [11]. Despite the agreement at high transmissions it is expected that this calculation underestimates p for lower

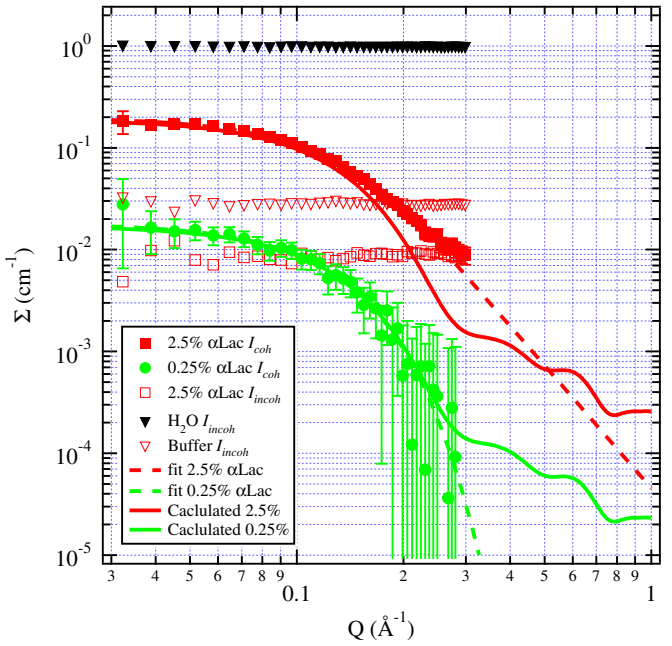

Fig. 4. Results of the PA measurement. Shown are curves for the coherent scattering of the alpha-lactalbumin sample at 2.5% and 0.25% concentrations, red solid squares, and green solid circles respectively. Also shown is the scattering from the deuterated buffer, open red triangles, and the incoherent scattering for the 2.5% sample, open red squares. The black closed triangles are the incoherent scattering from the 1 mm H_2O sample. The dashed lines are Beucage fits[24], with the background held to 0 and the solid lines are the CRYSON curves calculated in absolute units for the forward scattering for the two sample concentrations as described in the text. The X-scale is chosen to represent the full potential Q-range that will be accessible by our SANS instruments with future upgrades.

transmissions such as the H_2O sample. Regardless, the absolute values for the incoherent scattering cross sections of the deuterated buffer and H_2O sample are in good agreement with accepted values for these cross sections given the crude nature of this estimate. We note that for the determination of the values of N_{incoh} the inelastic effects as measured do not cause significant errors, as it should be on the 2 % level. Especially for the case of the H_2O sample, the multiple scattering corrections are much larger than the inelastic corrections. Regardless for the given H_2O I_{incoh} we used the corrected analyzing efficiency of $A_0 = 85.6$ % .

Shown also in figure 5 are the corresponding scattering curves for the equivalent unpolarized measurement obtained simply by summing the spin flip and non spin flip scattering. We also did a normal unpolarized measurement which gave the equivalent information. One can see the utility of the method, especially in the ability to obtain a clear scattering curve for the 0.25% Lactalbumin sample. Also on the graphs are the calculated scattering intensities. These calculated curves were obtained from the quoted structure of monomeric alpha-lactalbumin 1ALC.pdb [19] using the program CRYSON [20, 21] which is suitable for evaluating solution scattering from macromolecules with known molecular structures. The program uses a multi-pole expansion of the scattering amplitudes to calculate the spherically averaged scattering pattern and takes into account the hydration shell. Given the known atomic coordinates it can predict the solution scattering curve(s).

Theoretical calculation for the forward intensity $I(0)$ was performed according to [22]:

$$I(0) = \frac{cMK^2}{N_a} \tag{9}$$

Where c is the concentration of the solute (protein) in g/cm^3, M is the molecular weight of the solute (M (alpha-lactalbumin) = 16501 g/mol), N_a is the Avogadro Number (6.022E23 mol^{-1}), and K^2 is the square of the contrast between the solute and the solvent or, for instance, protein and the buffer and is calculated as

$$K^2 = (\rho_{protein} - \rho_{buffer}.V_p)^2 \tag{10}$$

Where $\rho_{protein}$ is the scattering length density of the protein, ρ_{buffer} is the scattering length density of the buffer and V_p is the specific volume of the protein (V_p (alpha-lactalbumin)= 0.735 cm^3/g according to [23]).

The calculated forward intensities match the measured data well for the respective concentrations and no scaling to these curves is made. Finally, also shown are Beaucage/Guinier fits [24] of the respective data.

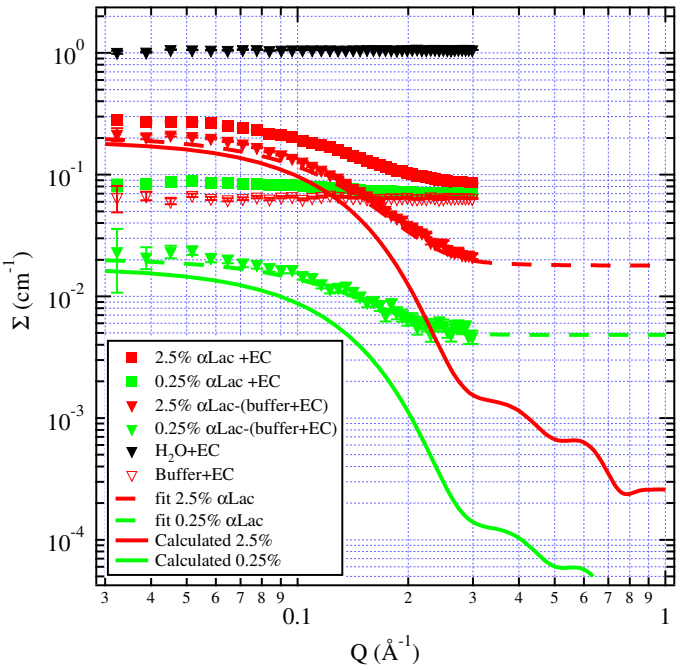

Fig. 5. Equivalent unpolarized data obtained by adding the two spin states. The respective curves are described in the legend. EC stands for empty cell which was not subtracted from the data separately. Equivalent data was also obtained with a standard unpolarized measurements but is not shown here.

Perhaps we observe a difference in the two scattering curves as may be expected given what is observed with WAXS measurements. However this must be confirmed and compared to results from other methods. Further, an improved installation should be completed in order to increase the Q range of our measurements into the high-Q regime between 0.2 to 1 Å^{-1} where the diffraction effects from internal structure and dynamics are expected to be more clearly observed.

4. Future plans for a dedicated polarization analysis device for JCNS SANS (KWS1, KWS2)

In order to make such measurements routine on the JCNS SANS instrumentation we have been working on an ultra compact in-situ ^{3}He polarizer. When complete this polarizer will allow polarization analysis for samples at low magnetic field and provide full detector coverage for KWS1 or KWS2 [9, 25] at the minimum detector distance. Special care was taken to minimize the length of this device because the minimum detector distance is about 80 cm from the front of the detector tank, thus any additional separation between the sample and detector would cause a noticeable loss in Q-range. The solution we arrived at has a total length of only 18 cm making the minimum detector to sample distance one meter when the device is placed in front of the detector tank in the sample environment area. The system will use a relatively small, 6 cm diameter ^{3}He cell, which due to the close placement to the entrance aperture of the magnetic cavity, shown in the figure 6, can provide analysis over the entire detector area. As can be seen there will be room for standard sample changers to be used, while maintaining a sample to cell distance of about 3 cm. The system will have AFP flipping capability to reverse the polarization direction of the ^{3}He while performing continuous optical pumping of the ^{3}He cell. Finally, in order to achieve the eventual 1 Å^{-1} Q-coverage, there are plans to ”tilt” the velocity selector in order to allow operation at a neutron wavelength of 3Å whereas the current minimum wavelength is 4.55 Å . However in this case the incident beam polarization must also be revised as the current transmission super mirror is optimized for the current beam parameters.

5. Conclusion

We have shown the feasibility of using a ^{3}He spin filter cell to perform polarization analysis for biological samples with SANS. The results look encouraging. Further work will be done to ensure inelastic effects

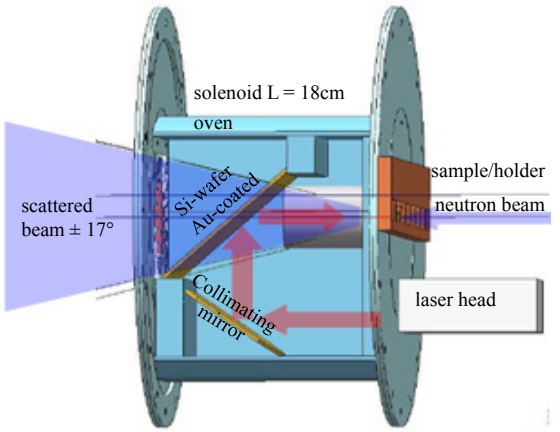

Fig. 6. A cutaway drawing showing the inside of the system under construction for in situ pumping. The cylinder and coil of the 17cm long solenoid and the cover of the SEOP oven are hidden to see the main components. The neutron beam is indicated by the violet arrow and enters from the right side through a 1.5 cm square entrance aperture. The scattered beam exits through a gold coated Si-wafer optical mirror-neutron window, after transmitting the ^{3}He cell, to the left. The laser head and narrowing optics are located outside of the cavity below the neutron beam indicated by the white box. Final expansion of the laser beam (optics not shown) will take place inside the magnetic cavity with the path of the laser beam indicated by the red arrows. All of the internal components are inside an oven which will be heated with electrical heaters to the approximately 200°C temperature required for SEOP.

are being properly accounted for and to insure that multiple scattering is being properly corrected when necessary. Eventually the results will be rigorously compared with measurements obtained using other methods such as WAXS or NSE. Finally we are continuing work to finish prototyping dedicated ^{3}He polarizers to be used on the JCSN SANS instrumentation. We thank Tobias Theissemann and Denis Korolkov for work on control software used on the ^{3}He analyzer cell [26], and note support of Z. Salhi by the German contribution to the ESS design update in work package K3. Additional portions of this work received support through the European Commission under the 7th Framework Programe through Key Action: Strengthening the European Research Area, Research Infrastructures. Contract no: CP-CSA_INFRA-2008-1.1.1 Number 226507-NMI3.

References

[1] Makowski L., Rodi D.J. Mandava S. Mihn D., Gore D., and Fischetti R.F., J. Mol. Biol **375**, 529-546 (2008).
[2] Makowski L. J. of Structural and Functional Genomics **11**, 9-19 (2010)
[3] Lal J., Fouquet P., Maccarini M., Makowski L., J. Mol. Biol. **397** 423-435 (2010).
[4] Fischer J. Biehl R., Hoffmann, B., and Richter D., European Biophysics J. with Biophysics Lett. **40** Supplement 1, 207-207 (2011)
[5] Sill C. Biehl R., Hoffmann B., and Richter D., European Biophysics J. with Biophysics Lett. **40** Supplement 1, 209-210 (2011)
[6] Rubinson K.A., Stanley C., Krueger S., J. App. Crystol. **41**, 456-465 (2008).
[7] Ioffe A., Babcock E., Mattauch S., Pipich V., Radulescu A., Appavou M.S., Chinese J. of Phys. **50** Special Issue, 137-154 (2012).
[8] Moon R.M., Riste T., Koehler W.C., Phys. Rev. **181**, 920- (1969)
[9] http://www.fz-juelich.de/jcns/EN/Leistungen/Instruments2/Structures/KWS2/_node.html.
[10] Ghosh R.E., Rennie A.R., Inst. of Phys. Conf. Series **107**, 233 (1990).
[11] Gentile T.R., Jones G.L., Thompson A.K., Barker J., Glinka C.J., Hammouda B., Lynn J.W., J. Appl. Crystol. **33** 771-774, (2000).
[12] McKetterick T.J., Boag S., Stewart J.R., Frost C.D., Skoda M.W.A., Parnell S.R., Babcock E., Physica B-Condensed Matter **406**, 2436-2438 (2011).
[13] Chen W.C., et. al. Proceedings of Polarized Neutrons in Condensed Matter Investigations, PNCMI 2012 Paris, this issue.
[14] Ioffe A., Feoktzsov A., Starringer S., Radulescu A., Babcock E., Salhi Z., Proceedings of Polarized Neutrons in Condensed Matter Investigations, PNCMI 2012 Paris, this issue.
[15] P. Calmettes, D. Durand, M. Desmadril, P. Minard, V. Receveur, and J.C. Smith, Biophysical Chemistry **53**, 105-114 (1994).
[16] D.R. Lide Ed., CRC Handbook of chemistry and physics, 80th Ed. (CRC Press, Boca Raton, 1999).
[17] T.E. Chupp, K.P. Coulter, M. Kandes, et. al., Nuclear Instr. and Meth. A, **574**, 500-509 (2007).
[18] Pipich V., iffwww.iff.kfa-juelich.de/ pipich/dokuwiki/doku.php/qtikws.
[19] Acharya, K.R., Stuart, D.I., Walker, N.P., Lewis, M., and Phillips, D.C. J. Mol. Biol. **208**, 99-127 (1989).
[20] Svergun D.I., Richard S., Koch M.H.J., Sayers Z., Kuprin S., Zaccai G. Proc. Natl. Acad. Sci. USA **95**, 22672272 (1998).
[21] Hura G.L., Menon A.L., Hammel M., Rambo R.P., Poole F.L., Tsutakawa S.E., Jenney F.E. Jr., Classen S., Frankel K.A., Hopkins R.C. et al. Nat. Methods **6**, 606612 (2009).
[22] Zaccai G. and Jacrot B., Ann. Rev. Biophys. Bioeng. **983 2**, 39-57 (1983).
[23] Bu Z., DA. Neumann D.A., Lee S-H., Brown CM. Engelman DM. and Han C.C. /bf JORNAL (2000).
[24] G. Beaucage, J. Appl. Crystol. **28**, 717-728 (1995).
[25] http://www.fz-juelich.de/jcns/EN/Leistungen/Instruments2/Structures/KWS1/_node.html
[26] https://github.com/pyfrid